NASA TECHNICAL MEMORANDUM

NASA TM X-67881

NASA TM X-67881

EFFECT OF RANDOMLY FLUCTUATING PRESSURE GRADIENTS, WITH ARBITRARILY SPECIFIED POWER SPECTRUM AND PROBABILITY DENSITY, ON FLOW IN CHANNELS

by Morris Perlmutter
Lewis Research Center
Cleveland, Ohio

TECHNICAL PAPER proposed for presentation at
The Symposium on Turbulence in Liquids
sponsored by the University of Missouri
Rolla, Missouri, October 4-6, 1971

EFFECT OF RANDOMLY FLUCTUATING PRESSURE GRADIENTS, WITH ARBITRARILY SPECIFIED POWER SPECTRUM AND PROBABILITY DENSITY, ON FLOW IN CHANNELS

by Morris Perlmutter

Lewis Research Center
National Aeronautics and Space Administration
Cleveland, Ohio

E-6393

ABSTRACT

A randomly fluctuating longitudinal pressure gradient of a non-Gaussian form and arbitrary power spectrum will cause a randomly fluctuating velocity to be superimposed on the steady incompressible flow in a channel. Pressure-gradient and velocity correlations, frequency response functions and system power loss are calculated. Numerical random pressure gradient signals were generated using Fourier series expansion, with random picking of discrete Fourier spectrum values and a nonlinear no memory transformation. Numerical values of the velocity signal were then calculated by linear transformation of the pressure-gradient signal. Pressure-gradient and velocity signals were compared for difference in amplitude, frequency, time lag, and probability distribution functions.

INTRODUCTION

The study of random fluctuations in engineering systems is receiving increasing attention. This is because practically all physical systems have some randomness which at times can cause the system behavior to be drastically different from the steady case.

The analysis of these stochastic problems is difficult, and usually only certain statistically averaged properties are obtained, such as the autocorrelation, which give only part of the information concerning the system. With the development of the high speed electronic computor it has become

feasible to study the random behavior of systems numerically, especially since the development of the fast Fourier transform algorithm which is a numerical method of rapidly taking Fourier transforms. This numerical calculation with random signals allows any statistical property of the signal to be calculated e.g. probability distribution function, by the appropriate numerical techniques.

The present analysis describes the effect of a randomly fluctuating pressure gradient on the flow of an incompressible fluid in a channel (fig. 1) both analytically and numerically. A pressure-gradient signal having an arbitrarily specified probability distribution and power spectrum is generated numerically. From this the velocity signal can be calculated. The velocity signal can then be analyzed for its probability distribution function, power spectrum and any other characteristic of interest. Analytical results are computed where possible and the numerical and analytical results are compared.

In a previous analysis (ref. 1) this same flow problem was studied for the case where the pressure gradient fluctuations were restricted to a Gaussian (normal) probability distribution. Since the fluid velocity was linearly related to the pressure gradient, the velocity fluctuations would also be normally distributed. Therefore all the velocity characteristics would be given by the autocorrelation function of the velocity. However, for the non-Gaussian pressure gradient the velocity distribution is also non-Gaussian and cannot be characterized by the autocorrelation function alone. By use of a numerical method however the velocity signal is generated numerically and all its statistical characteristics can be found by the appropriate statistical analysis of the signal.

Tien and Lienhard studied a similar problem for pipe flow (ref. 2) and included the effect of turbulent eddy diffusivity in Ref. 3. However only the autocorrelation results were given. This would not be sufficient to fully characterize a non-Gaussian system.

As shown in Ref. 1 it is possible to generate numerically a Gaussian signal with a given power spectrum. Then by a nonlinear, no memory transformation this initial signal can be transformed into a pressure gradient signal with the desired non-Gaussian probability distributions and associated

power spectrum. From this, through a linear transformation the velocity signal can be found and analyzed for its statistical properties. This process is outlined in Fig. 2.

ANALYSIS

In the present case we are interested in generating a random pressure-gradient signal with a non-Gaussian probability distribution. To do so we must first generate a Gaussian signal then transform it to the desired signal. The method used is illustrated in Fig. 2. A Gaussian signal $w(t)$ with a specified spectrum is subjected to a suitable nonlinear no memory transformation such that a pressure-graidient signal γ is obtained having the desired probability density function p_γ. This transformation can be written as $\gamma = g(w)$. We can relate the distribution functions of γ and w by the well known relation

$$\int_{g(-\infty)}^{g(w)} p_\gamma \, d\gamma = \int_{-\infty}^{w} p_w \, dw \tag{1}$$

The power spectrum of the generated signal $S_{ww}(\omega)$ must be specified so that the nonlinear transformation, $\gamma = g(w)$, will have the desired power spectrum $S_{\gamma\gamma}$.

The autocorrelation of the generated w signal, which is the Fourier transform of the power spectrum, is obtained in terms of the desired pressure-gradient signal autocorrelation as follows.

Generated Signal Autocorrelation

We can write the pressure-gradient signal autocorrelation as follows (ref. 4, pg. 51)

$$R_{\gamma\gamma} = E\left[\gamma_1(t_1)\gamma_2(t_2)\right] = \int_{-\infty}^{+\infty}\int g(w_1)g(w_2)p_{w_1w_2} \, dw_1 \, dw_2 \tag{2}$$

where $p_{w_1w_2}$ is the normal bivariate distribution given by

$$p_{w_1 w_2} = \frac{\exp\left\{ -\left[w_1^2 - 2\rho_{ww} w_1 w_2 + w_2^2\right] \Big/ 2\sigma_w^2 (1 - \rho_{ww}^2) \right\}}{2\pi\sigma_w^2 (1 - \rho_{ww}^2)^{1/2}} \tag{3}$$

ρ_{ww} is the normalized autocorrelation R_{ww}/σ_w^2, and σ_w^2 is the variance.

It has been shown in Ref. 4 (p. 52) that the $R_{\gamma\gamma}$ can be written as an algebraic function of ρ_{ww}. Then for a known Gaussian signal, p_w, and known transformation, $\gamma = g(w)$; the autocorrelation ρ_{ww} of the input Gaussian signal that, after the nonlinear transformation to the pressure signal, will have the desired autocorrelation $R_{\gamma\gamma}$ can be calculated by iteration.

A simpler method of calculating ρ_{ww} is given in Ref. 5 for the case where the nonlinear transformation between γ and w is given in the specified form,

$$\gamma = g(w) = \frac{1}{K\sigma_w \alpha \sqrt{2\pi}} \int_0^w e^{-u^2/2\sigma_w^2\alpha^2}\, du \tag{4}$$

$$= \frac{1}{K\sqrt{\pi}} \int_0^{w/\sqrt{2}\sigma_w\alpha} e^{-\eta^2}\, d\eta$$

The K and α are adjustable parameters that allow a wide variety of relationships between γ and w to be approximated.

The plot of γ versus w given by Eq. (4) are plotted in Fig. 3. Although all values of w are possible the values of γ are restricted between $\pm 0.5/K$. The value of K thus determines the cutoff amplitude of γ. For $\alpha = 0$ all values of w transform to $\pm 0.5/K$ giving a rectangular wave for γ. As α becomes large, Eq. (4) reduces to $K\gamma \to w/(\sqrt{2\pi}\,\alpha\sigma_w)$ so that $\gamma \propto w$.

From Eqs. (1) and (4) we can write the distribution of γ as

$$\frac{p_\gamma}{K} = \alpha\, e^{-w^2(1-\alpha^{-2})2\sigma_w^2} \tag{5}$$

Eq. (5) can be evaluated by finding w for a specified value of γ using Eq. (4). Then p_γ/K can be evaluated from Eq. (6). The plot of p_γ/K versus γK is shown in Fig. 4. Significantly different probability distributions p_γ can be obtained for different values of α and K.

If $\gamma = g(w)$, given by Eq. (4), is substituted into Eq. (2), then as shown in Ref. 5, $R_{\gamma\gamma}$ is given by

$$R_{\gamma\gamma} = \frac{1}{2\pi K^2} \sin^{-1}\left(\frac{\rho_{ww}}{1+\alpha^2}\right) \tag{6}$$

This can be evaluated at $\tau = 0$ to give

$$R_{\gamma\gamma}(\tau = 0) = \frac{\theta}{2\pi K^2}\ ;\ \text{where}\ \ \theta = \sin^{-1}\left(\frac{1}{1+\alpha^2}\right) \tag{7}$$

We can now write

$$\rho_{\gamma\gamma} = \frac{1}{\theta} \sin^{-1}\left(\frac{\rho_{ww}}{1+\alpha^2}\right) \tag{8}$$

which can be inverted to

$$\rho_{ww} = (1+\alpha^2) \sin\left[\theta \rho_{\gamma\gamma}\right] \tag{9}$$

This gives the needed Gaussian autocorrelation ρ_{ww} so that the nonlinear transformation given by Eq. (4) will give the desired pressure gradient autocorrelation $\rho_{\gamma\gamma}$.

Pressure Gradient Autocorrelation

A common form of random fluctuation is called a stationary Gaussian Markoff Process. This gives an exponential form of the pressure gradient autocorrelation (ref. 6, pg. 215).

$$R_{\gamma\gamma} = \sigma_\gamma^2 e^{-\Lambda|T|} = \sigma_\gamma^2 e^{-\lambda|\tau|} \tag{10}$$

where the rate of fluctuation Λ and the time span T have been nondimensionalized by

$$\lambda = \frac{\Lambda d^2}{\nu}\ ;\ \tau = \frac{T\nu}{d^2} \tag{11}$$

where ν is the fluid kinematic viscosity and d is the distance across the channel. The λ is a dimensionless measure of the fluctuation rate. It can

also be considered the inverse of the dimensionless characteristic decay time of the autocorrelation. The larger the λ value, the greater the fluctuation rate of the pressure gradient signal. The fluctuation rate can be characterized by the number of crossings of the o value of the signal per unit time. The quantity σ_γ^2 is the mean square value of the pressure fluctuations $\langle \gamma^2 \rangle$. It also can be considered the integrated power spectrum of the pressure signal since

$$R_{\gamma\gamma}(\tau=0) = \sigma_\gamma^2 = \int_{-\infty}^{+\infty} S_{\gamma\gamma}\, df \tag{12}$$

where $S_{\gamma\gamma}$ is the power spectrum and f is the frequency. The larger the σ_γ^2 value, the larger the magnitude of the pressure fluctuations.

The autocorrelation of the generated signal from Eq. (9) for the case of the stationary markoff pressure gradient signal becomes

$$\rho_{ww} = (1 + \alpha)^2 \sin\left[\theta\, e^{-\lambda|\tau|}\right] \tag{13}$$

The dimensionless autocorrelations ρ_{ww} and $\rho_{\gamma\gamma}$ are shown in Fig. 5.

Since the power spectrum $S_{\gamma\gamma}$ is the Fourier transform of the autocorrelation, $R_{\gamma\gamma}$, we can write the dimensionless power spectrum of the pressure gradient as

$$\psi_{\gamma\gamma} = \frac{S_{\gamma\gamma}}{R_{\gamma\gamma}(0)} = \frac{2\lambda}{\lambda^2 + \omega^2} \tag{14}$$

where ω is the angular Fourier frequency, $2\pi f$. The generated signal's dimensionless power spectrum is given by

$$\psi_{ww} = (1 + \alpha^2) \int_{-\infty}^{+\infty} \sin\left[\theta e^{-\lambda|\tau|}\right] e^{-\omega\tau}\, d\tau \tag{15}$$

Expanding $\sin\left[\theta e^{-\lambda|\tau|}\right]$ in a series gives, for the present pressure gradient markoff process case,

$$\psi_{ww} = (1 + \alpha^2) \sum_{n=1,3,5} \frac{\theta^n}{n!} (-1)^{(n+3)/2} \frac{2(\lambda n)}{\left[(n\lambda)^2 + \omega^2\right]} \tag{16}$$

Generation of a Gaussian Random Signal by Model Sampling

The Gaussian random signal w(t) can be obtained as shown in Ref. 1 by writing the signal as an inverse discrete Fourier Transform, $w_{\omega n}$, where n

are integer values. It follows that the discrete Fourier spectra can be considered a Gaussian random variable with a zero mean and a variance that can be related to the power spectrum. We can use a random sampling procedure to pick the discrete Fourier spectrum values from the appropriate distribution. Then by use of "fast Fourier transforms" we can obtain the signal values at discrete points. This detailed procedure is as follows.

As shown in Ref. 1 the power spectrum, S_{ww}, of a signal w which has a Fourier spectrum w_ω can be written as

$$S_{ww} = \lim_{T_p \to \infty} \frac{1}{T_p} \left[\left\langle w_\omega w_\omega^* \right\rangle \right] = \lim_{T_p \to \infty} \frac{1}{T_p} \left[\left\langle w_{\omega R}^2 \right\rangle + \left\langle w_{\omega I}^2 \right\rangle \right] \tag{17}$$

Where w_ω^* is the complex conjugate of the Fourier spectrum. The $w_{\omega R}$ and $w_{\omega I}$ are the real and imaginary components of the Fourier spectrum. The term $\langle . \rangle$ denotes ensemble averages. Thus the power spectrum can be related to the average of the squares of the Fourier spectrum of the random signal.

Discrete Fourier transform. - When a signal is to be analyzed on a digital computer it is the discrete Fourier spectrum rather than the continuous spectrum that must be considered. If the Fourier spectrum w_ω is band limited so that $w_\omega \approx 0$ for $f > f_M$ we can write (ref. 7, pg. 152)

$$w_\omega = \sum_{n=-\infty}^{+\infty} C_n e^{-i2\pi nf/f_p} \; ; \; f_p > 2f_M \; ; \; \frac{-f_p}{2} < f < \frac{f_p}{2} \tag{18}$$

where

$$c_n = \frac{1}{f_p} \int_{-f_p}^{+f_p} w_\omega e^{in2\pi f/f_p} \, df \tag{19}$$

Since $w_\omega = 0$ for $f > f_M$ we can see that, using $F^{-1}( )$ to denote inverse transforms, then

$$c_n f_p = F^{-1} \left[w_\omega \right] = w_n \left(t = \frac{n}{f_p} \right) \tag{20}$$

Thus knowing w at discrete values of t allows w_ω to be evaluated from Eqs. (18) and (20). Then by taking the inverse continuous Fourier transform of w_ω we obtain w at all times. Since we assumed $t = n/f_p = n\Delta t$ we can see that

$$\Delta t = \frac{1}{f_p} \leq \frac{1}{2f_M} \tag{21}$$

which is sometimes called the Nyquist interval.

If we take $N + 1$ samples of w_n we can write Eq. (18) as

$$w_{\omega,k}(k\Delta f) = \frac{1}{f_p} \sum_{n=-N/2}^{+N/2} w_n e^{-2i\pi nk/N} \tag{22}$$

Since $f_p = 1/\Delta t = N/T_p$ we can write the above as

$$\left(\frac{w_{\omega k}}{T_p}\right) = \frac{1}{N} \sum_{n=-N/2}^{+N/2} w_n e^{-i2\pi nk/N} \tag{23}$$

As shown in Ref. 1, this can be considered a discrete Fourier transform. The inverse discrete Fourier transform can then be written as

$$w_n = \sum_{k=-N/2}^{N/2} \left(\frac{w_{\omega k}}{T_p}\right) e^{i2\pi kn/N} \tag{24}$$

So that Eqs. (23) and (24) form a discrete Fourier transform pair that are approximations to the continuous Fourier transform pair.

Fast Fourier transforms. - A numerical method has been developed, called the fast Fourier transform (ref. 8), for evaluating discrete Fourier transforms in a very efficient manner on a digital computer. One implementation readily available is the IBM-scientific subroutine package called HARM/DHARM. Many others are available.

Model sampling to generate Gaussian signal. - We can expand $w_{\omega k}$ in Eq. (24) into real and imaginary parts. Since w_n is a real function the imaginary term must be zero and so $w_{\omega nR}$ must be an even function around $n = 0$ while $w_{\omega nI}$ is an odd function around $n = 0$. Then we can write

$$w_k = \frac{1}{T_p} \sum_{n=-N/2}^{+N/2} \left(w_{\omega nk} \cos \frac{2\pi nk}{N} - w_{\omega nI} \sin \frac{2\pi nk}{N} \right) \tag{25}$$

It has been shown in Ref. 1 that for a Gaussian random process $w_{\omega nk}$ and $w_{\omega nI}$ are normally distributed, independent, random variables with zero mean and variance given by

$$\begin{aligned} \left\langle w^2_{\omega nk} \right\rangle = \left\langle w^2_{\omega nI} \right\rangle = \left\langle w^2_{\omega n} \right\rangle \qquad & n \neq 0 \\ \left\langle w^2_{\omega nI} \right\rangle = 0 \qquad & n = 0 \end{aligned} \tag{26}$$

Then from Eqs. (17) and (26) we can obtain

$$S_{ww}\Big|_{\omega = n2\pi/T_p} = \begin{cases} \dfrac{2}{T_p} \left\langle w^2_{\omega n} \right\rangle & n \neq 0 \\ \dfrac{\left\langle w^2_{\omega n} \right\rangle}{T_p} & n = 0 \end{cases} \tag{27}$$

We can generate the values of $w_{\omega nk}$ and $w_{\omega nI}$ by first writing their joint Gaussian probability distribution

$$p(w_{\omega nR}, w_{\omega nI}) = \frac{1}{2\pi \left\langle w^2_{\omega n} \right\rangle} \exp \left\{ - \frac{1}{2 \left\langle w^2_{\omega n} \right\rangle} (w^2_{\omega nR} + w^2_{\omega nI}) \right\} \tag{28}$$

Following the procedure in Ref. 1 we can randomly sample values from the above distribution with the equations

$$\begin{aligned} w_{\omega nR} &= \left(2 \left\langle w^2_{\omega n} \right\rangle \right)^{1/2} (-\ln R_r)^{1/2} \cos 2\pi R_\theta \\ w_{\omega nI} &= \left(2 \left\langle w^2_{\omega n} \right\rangle \right)^{1/2} (-\ln R_r)^{1/2} \sin 2\pi R_\theta \end{aligned} \tag{29}$$

where R_θ and R_r are two different random numbers picked from a uniform distribution that is constant between 0 and 1. These values can readily be generated on a digital computer. Recalling that $w_{\omega nR}$ is an even function and $w_{\omega nI}$ is an odd function, in the particular fast Fourier program used (HARM/DHARM), we need only find $w_{\omega nR}$ and $w_{\omega nI}$ from $n = 0$ to $N/2$. Then $w_{\omega, (N/2)+1, R} = w_{\omega, (N/2)-1, R}$, etc. Similarly $w_{\omega, (N/2)+1, I} = -w_{\omega, (N/2)-1, I}$, etc. The value of $w_{\omega, 0, I}$ is equal to zero.

After finding the values of $w_{\omega,n}$ we can substitute them into Eq. (25) and using the fast Fourier transform routine find the values of w_k.

The sample mean $\overline{w}$ and the sample variance $\overline{w^2}$ are then found from the w_k values. With this the value of w_k can be normalized, $w'_k = (w_k - \overline{w})/(\overline{w^2})^{1/2}$. Then the distribution and autocorrelation are found by using available subroutines on the values of w'_k.

The example case is carried out using the power spectrum S_{ww} given by Eq. (16). The normalized signal w' is plotted in Fig. 6 for a λ value of 1.

In Fig. 7 the cumulative distribution function of w' obtained numerically is plotted along with the Gaussian cumulative distribution function with good agreement. This shows that the w' is normally distributed as expected.

The numerical results for the autocorrelation of the w' signal is shown in Fig. 5 and compares well with its theoretical result, although the agreement seems to fall off for large time lag τ.

Generation of γ signal from w signal. - To transform the w signal into the pressure gradient signal γ we use Eq. (4) which allows us for each $w_n(n\Delta t)$ to calculate a $\gamma_n(n\Delta t)$ value for each n from 0 to N. This gives the pressure gradient signal with the desired probability distribution and autocorrelation. This signal is normalized to γ' and shown in Fig. 6. Since the normalized pressure gradient signal cannot have any values larger than $(0.5/\sigma_\gamma)$ we can see this cutoff in Fig. 6. It can be seen from Fig. 4 that the pressure cutoff is at lower values of γ' for smaller values of λ since the normalizing factor σ_γ increases for decreasing α, see Fig. 4. The cumulative distribution of the γ' signal is shown in Fig. 7 where it can be seen to agree with the analytical result. The autocorrelation of the γ' signal is shown in Fig. 5 and also agrees with the analytical result.

Relation Between Velocity Signal and Pressure Signal

This procedure follows the analysis in Ref. 1. To calculate the fluid velocity signal from the pressure gradient signal we must first solve the momentum equation. For viscous incompressible flow between parallel plates with constant properties in the fully developed flow region (see fig. 1) the

momentum equation can be written as

$$\frac{\partial U}{\partial T} = -\frac{1}{\rho} P(T) + \nu \frac{\partial^2 U}{\partial Y^2} \tag{30}$$

We can let the velocity and the pressure gradient consist of a steady part and a nonsteady part $U = U_s + U_t$; $P = P_s + P_t$. Normalizing as follows

$$u_s = -\frac{\nu\rho U_s}{d^2 P_s} \quad v = -\frac{\nu\rho U_t}{d^2 P_s} \quad y = \frac{Y}{d} \quad t = \frac{\nu T}{d^2} \quad \gamma = \frac{P_t}{P_s}$$

we can obtain

$$u_s = \frac{y - y^2}{2} \; ; \; \frac{\partial v}{\partial t} = \gamma + \frac{\partial^2 v}{\partial y^2} \tag{31}$$

The solution for v as shown in Ref. 1 is given by

$$v = \int_{-\infty}^{+\infty} h(\theta, y)\gamma(t - \theta)d\theta = \int_{\delta=\infty}^{t} h(t - \delta, y)\gamma(\delta)d\delta \tag{32}$$

where h is the weighting function given by

$$\left.\begin{aligned} h(\theta) &= \sum_{m=1,3,5}^{\infty} Y_M \, e^{-M^2(\theta)} \qquad \text{for } \theta > 0 \\ h(\theta) &= 0 \qquad\qquad\qquad\qquad\quad \text{for } \theta < 0 \end{aligned}\right\} \tag{33}$$

where $M = m\pi$. The Fourier transform of Eq. (32) is given by

$$v_\omega = \gamma_\omega H \tag{34}$$

where

$$H = \sum_{m=1,3,5}^{\infty} \frac{Y_M}{M^2 + i\omega} = H_R + iH_I = |H| \, e^{-i\varphi} \tag{35}$$

and $Y_M = 4 \sin My/M$. The H is sometimes called the system transfer function. We can write the real and imaginary parts of H as

$$H_R = \sum_{m=1,3,5} \frac{Y_M M^2}{M^4 + \omega^2}\,; \quad H_I = -\omega \sum_{m=1,3}^{\infty} \frac{Y_M}{M^4 + \omega^2} \tag{36}$$

The gain factor of the system function is given by $|H| = (H_R^2 + H_I^2)^{1/2}$ and the phase factor of the system function by $\varphi = \tan^{-1}(H_I/H_R)$. The gain and phase factors are plotted in Fig. 8. As can be seen in the figure, for small values of angular frequency ω the system frequency transfer function approaches the distortionless limit $|H| = |H|_d$; $\varphi_d = -\omega t_l$ to give

$$H = |H|_d \, e^{+i\omega t_l}$$

Then taking inverse Fourier transforms of Eq. (34)

$$v = |H|_d \int_{-\infty}^{+\infty} \gamma_\omega \, e^{+i\omega t_l} \, e^{i\omega t} \, \frac{d\omega}{2\pi} = |H|_d \gamma(t + t_l) \tag{37}$$

This shows for very low frequency, $\omega \to 0$, the velocity signal duplicates the pressure signal but is a fraction $|H|_d$ of the pressure signal amplitude. The velocity signal lags the pressure signal by a time increment t_l. We can find the limiting value of t_l as $\omega \to 0$ as 0.0781.

The gain factor decreases in magnitude close to the wall. This shows that the magnitude of the velocity fluctuations close to the wall is smaller than near the center of the channel. The percent decrease in the gain factor at the higher frequencies is larger near the center of the channel so that there will be relatively more damping of the higher frequency velocity fluctuations near the center of the channel than near the wall. The phase factors are smaller near the channel wall than near the center showing that there is a smaller signal lag of the velocity signal behind the pressure signal closer to the wall.

The cross correlation of the pressure and velocity fluctuations can be obtained from Eq. (32) as

$$R_{\gamma v}(\tau) = \left\langle \gamma(t) v(t + \tau) \right\rangle = \int_0^\infty h(\theta, y) \left\langle \gamma(t) \gamma(t + \tau - \theta) \right\rangle d\theta = \int_0^\infty h(\theta y) R_{\gamma\gamma}(\tau - \theta) d\theta \tag{38}$$

where R is the time lag. Since the cross spectrum is the Fourier transform of the cross correlation, by using the convolution theorem we can write

$$S_{\gamma v}(\omega) = H(\omega)S_{\gamma\gamma}(\omega) \tag{39}$$

We can find the velocity autocorrelation similarly as

$$R_{vv}(\tau) = \int_0^\infty h(\theta, y)R_{\gamma v}(\tau + \theta)d\theta \tag{40}$$

Then we can write the power spectrum as

$$S_{vv}(\omega) = H^*(\omega)S_{\gamma v}(\omega) = H^*(\omega)H(\omega)S_{\gamma\gamma}(\omega) = \left|H(\omega)\right|^2 S_{\gamma\gamma}(\omega) \tag{41}$$

The pressure-velocity cross correlation for the present case can be written using Eqs. (10), (33), and (38) as

$$R_{\gamma v}(\tau) = \begin{cases} \sigma_\gamma^2 \sum_{m=1,3,5}^{\infty} \left[Y_M/(M^2 - \lambda)\right]\left[e^{-\lambda\tau} - \left[2\lambda/(\lambda + M^2)\right]e^{-M^2\tau}\right] & \text{for } \tau \geq 0 \\ \sigma_\gamma^2 \sum_{m=1,3,5}^{\infty} Y_M\, e^{\lambda\tau}/(M^2 + \lambda) & \text{for } \tau < 0 \end{cases} \tag{42}$$

In a similar manner we can calculate the velocity autocorrelation from Eqs. (10), (33), and (40) as

$$R_{vv}(\tau) = \sigma_\gamma^2 \sum_{m=1,3}^{\infty}\sum_{m=1,3}^{\infty} \left[Y_M Y_{M'}\ (M'^2 - \lambda)\right]\left[e^{-\lambda\tau}/(\lambda+M^2) - \left(2\lambda/\left[\lambda+M'^2\right]\right)e^{-M'^2\tau}/(M^2+M'^2)\right] \tag{43}$$

The normalized power spectrums are plotted in Fig. 9. The pressure gradient spectrum from Eq. (14) for the stationary markoff process can be seen to have a lower frequency cutoff for lower values of λ or slower rates of fluctuations. The normalized velocity spectrums given by Eq. (41) are also shown and for the lower values of λ are close to the normalized pressure gradient spectrums and not strongly dependent on distance across the channel. However at the higher fluctuation rate, or large λ, the power spectrum of the velocity signal have more of the power concentrated at the lower frequency then the power

spectrum of the pressure gradient signal.

The mean square velocity, $\langle v^2 \rangle$, can be obtained from Eq. (43) since

$$\langle v^2 \rangle = R_{vv}(o, y) = \int_{-\infty}^{+\infty} S_{vv}\, df = \int_{-\infty}^{+\infty} |H(\omega)|^2 S_{\gamma\gamma}(\omega) df \tag{44}$$

The values of $\langle v^2 \rangle$ across the channel for different values of λ are shown in Fig. 10.

Since the gain factor is smaller near the wall ($y = 0.1$) compared to that at the centerline ($y = 0.5$), the mean square velocity is smaller near the wall as compared to the centerline. The mean square velocity goes to zero at the wall (fig. 10) as would be expected from the zero wall velocity boundary condition. The gain factor is greatest at the lower frequency and has a high-frequency cutoff (cf. fig. 8). Therefore for a given mean square pressure gradient value the maximum value of $\langle v^2 \rangle$ is found when the pressure gradient spectrum is a delta function at small ω. The minimum value of $\langle v^2 \rangle$ occurs if the pressure spectrum is a delta function at large value of ω.

Power Dissipation Due to Velocity Fluctuations

It is desirable to know how much additional power must be supplied to the flow system to maintain the same average flow rate for the fluctuating flow as compared to the steady flow case. As shown in Ref. 1, the external rate of work done by the pressure force w_e is equal to the sum of the rate of increase in kinetic energy K_e and the rate of dissipation of energy due to internal friction w_f. If we then take the ensemble average, the rate of change of the kinetic energy term will be zero because the process is stationary. We then have the external rate of work done by the pressure force w_e equal to the rate of dissipation of energy due to external friction w_f

$$-\langle \overline{U}P \rangle = \mu \int_0^1 \langle (\partial U/\partial Y)^2 \rangle dy \tag{45}$$

where $\overline{U}$ is the integrated value across the channel, $\int_0^1 U\, dy$.

To find the rate of dissipation of energy due to internal friction we can then write

$$w_f = - \left\langle \overline{UP} \right\rangle = - \overline{U}_s P_s - \left\langle \overline{U}_t P_t \right\rangle = w_{f,s} - \left\langle \overline{U}_t P_t \right\rangle \tag{46}$$

If we let $w_{f,s}$ be the rate of dissipation due to steady flow, the ratio of increased dissipation due to the unsteady flow over the steady flow dissipation can be written as

$$(w_f - w_{f,s})/w_{f,s} = \left\langle \overline{U}_t P_t \right\rangle / \overline{U}_s P_s = 12 \overline{R}_{\gamma v}(o) = 12 \int_{-\infty}^{+\infty} \overline{H} S_{\gamma\gamma} \, d\omega \tag{47}$$

Integrating Eq. (42) over y and substituting the result Eq. (51) give

$$(w_f - w_{f,s})/w_{f,s} = 96\sigma_\gamma^2 \sum_{m=1,3,5}^{\infty} 1/M^2(M^2 + \lambda) \tag{48}$$

This result is shown in Fig. 11 as a function of the fluctuating rate parameter λ. As λ becomes very large, that is, as fluctuations of the pressure gradient become very rapid, the frictional power loss reduces to the steady power loss. The frictional power loss increases with smaller values of λ, that is, with slower fluctuations of the pressure gradient. For a given mean square pressure gradient the maximum rate of power dissipation that can be achieved can be seen from Eq. (47) to be when $S_{\gamma\gamma}$ is a delta function at the maximum value of $\overline{H}$ which is at small ω. The minimum power dissipation occurs when $S_{\gamma\gamma}$ is a delta function at the minimum value of $\overline{H}$: i.e., ω large.

Calculating Velocity Signal From Pressure Signal

We can write the velocity signal as before (eq. (24))

$$v_n = \sum_{k=-N/2}^{N/2} \left(\frac{v_{\omega k}}{T_p} \right) e^{i2\pi kn/N} \tag{49}$$

From Eq. (34) we can write

$$v_{\omega n} = \left(H_n \Big|_{\omega_n = \frac{n2\pi}{T_p}} \right) \gamma_{\omega n} \tag{50}$$

The values of $\gamma'_{\omega n}$ can be obtained by taking the fast Fourier transform of γ'_n which were calculated previously. Then by use of Eq. (50) we can obtain the values for $v_{\omega n}$. The values of v_n are then obtained using the inverse fast Fourier transform. From these values the normalized values v'_n can be found. These are plotted in Fig. 12. When compared to the pressure signal it can be seen there is rounding of the sharp cutoff of the pressure signal. Fig. 7 shows the cumulative distribution of the velocity signal which can be seen to be similar in shape to the cumulative distribution of the pressure signal but tending towards the Gaussian cumulative distribution. The autocorrelation of the velocity signal is shown in Fig. 13 to agree fairly well with the theoretical results given by Eq. (43) but diverges somewhat for large lag times τ.

SUMMARY AND CONCLUSIONS

The effect of imposing a randomly fluctuating pressure gradient with a non-Gaussian probability distribution and an arbitrary spectrum on a fluid in a channel causes a randomly fluctuating velocity component to be superimposed over the steady flow. The mean value of the velocity fluctuation is zero. The mean square value of the velocity fluctuations which is a measure of the amplitude of the velocity fluctuations is highest in the center of the channel and reduce to zero at the wall. Also the slower the rate of the pressure gradient fluctuations the greater the amplitude of the velocity fluctuations.

The pumping power loss was increased by the flow fluctuations, the slower pressure gradient fluctuation rate giving the larger power loss.

The non-Gaussian random pressure gradient signal with a stationary mark-off power spectrum was obtained numerically by first generating a Gaussian signal with a specified power spectrum. This was generated by first choosing

random values of the coefficients of the discrete Fourier spectrum representation from a Gaussian distribution whose variance was obtained from the specified power spectrum. Taking fast Fourier transforms of the discrete Fourier spectrum gave discrete values of the Gaussian signal. This signal was then transformed through a nonlinear, no memory, relation to the desired non-Gaussian fluctuating pressure gradient signal. The velocity signal was obtained by first taking the fast Fourier transform of the pressure gradient signal and multiplying the resulting discrete Fourier spectrum by the system frequency response function. This gave the discrete velocity Fourier spectrum which was then fast Fourier transformed to the velocity signal. The numerical signals were then analyzed to obtain their correlations and frequency distribution functions.

The normalized velocity signals were close in value to the normalized pressure gradient signal but had a dimensionless time lag $\nu T/d^2$ of about 0.0781 for the lower pressure gradient fluctuation rates (small λ). At the higher rates of fluctuation of the pressure gradient signal (large λ) less of the high frequency fluctuations pressure gradient signal appear in the velocity signal. More so near the center of the channel rather than near the wall. Also the time lag of the velocity signal behind the pressure gradient signal is larger near the center of the channel then near the wall. The velocity signal tended to overshoot the upper limit of the pressure gradient signal.

The nondimensional cumulative probability distribution for the velocity signal is very close to the cumulative probability distribution for the pressure gradient at the low fluctuation rate (small λ). However at the higher values of λ the normalized cumulative probability distribution for the velocity approached the Gaussian cumulative probability distribution.

APPENDIX - SYMBOLS

a_n, b_n	complex coefficients
d	spacing between parallel plates
E	expected value
f	frequency
f_o	frequency increment, $1/T_p$
f_p	maximum frequency
F, F^{-1}	Fourier transform, inverse Fourier transform
H	frequency response function
$\|H\|$	gain factor
h	weighting function or impulse response function
i	unit imaginary number
M, M'	$m\pi$; $m'\pi$
N	number of samples
P	pressure gradient
p	probability distribution function
R_{xy}	correlation (x, y)
S	spectrum
T	time
T_p	period of record
t	dimensionless time, $\nu T/d^2$
Δt	time between sample
U	fluid velocity
u_s	steady dimensionless velocity, $-\nu\rho U_s/d^2 P_s$

v	transient dimensionless velocity, $-\nu\rho Ut/d^2P_s$
w	generated Gaussian signal
Y	coordinate across channel
Y_M	4 sin My/M
y	dimensionless coordinate across channel, Y/d
α	parameter (eq. (4))
β	constant; $\sin^{-1}(1/1 + \alpha^2)$
γ	dimensionless pressure gradient, P_t/P_s
θ	parameter given by Eq. (7)
Λ	measure of rate of fluctuation of pressure signal
λ	dimensionless measure of rate of fluctuation of pressure signal, $\Lambda d^2/\nu$
ν	kinematic viscosity
ρ_{xx}	normalized autocorrelation $R_{xx}/R_{xx}(0)$
σ^2	variance
τ	dimensionless time difference, $t_2 - t_1$
φ	phase factor
ψ	normalized power spectrum, S/R(0)
ω	angular frequency, $2\pi f$
( )	sample average
$\langle\ \rangle$	ensemble average
*	complex conjugate
'	normalized variable

Subscripts:

F	fundamental frequency or lowest frequency, $1/T_p$
H	related to frequency response function
I	imaginary
R	real
s	steady component
t	fluctuating component
γ	related to pressure signal
ω	Fourier spectrum

REFERENCES

1. Perlmutter, Morris: Randomly Fluctuating Flow in a Channel Due to Randomly Fluctuating Pressure Gradients. NASA TN D-6213, 1971.

2. Tien, C. L. ; and Lienhard, J. H.: Pressure-Flow Characteristics of Randomly Oscillating Pipe Flows. J. Appl. Mech., vol. 83, no. 3, Sept. 1961, pp. 463-465.

3. Lienhard, John H.; and Tien, C. L.: Randomly Oscillating Turbulent Channel Flows, Zeit. f. Angew, Math. Phys., vol. 15, no. 4, 1964, pp. 375-381.

4. Grenander, Ulf; and Rosenblatt, Murray: Statistical Analysis of Stationary Time Series. John Wiley & Sons, Inc., 1957.

5. Baum, R. F.: The Correlation Function of Smoothly Limited Gaussian Noise. IRE Trans. on Information Theory, vol. IT-3, no. 3, Sept. 1957, pp. 193-197.

6. Bendat, Julius S.; and Piersol, A. G.: Measurement and Analysis of Random Data. John Wiley & Sons, Inc., 1966.

7. Hsu, H. P.: Fourier Analysis. Simon & Schuster, Tech. Outline Series, 1970.

8. Gentleman, W. M.; and Sande, S.: Fast Fourier Transforms - For Fun and Profit. AFIPS Conference Proceedings. Vol. 28, 1966, pp. 563-578.

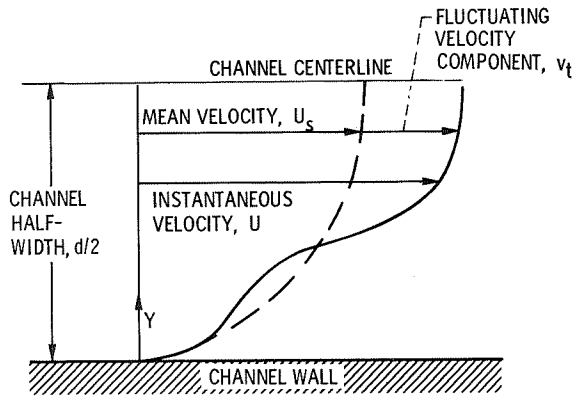

Figure 1. - Parallel plate channel flow model.

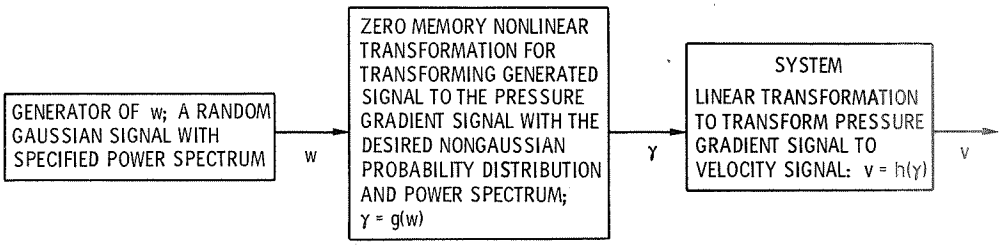

Figure 2. - Flow chart of numerical analysis.

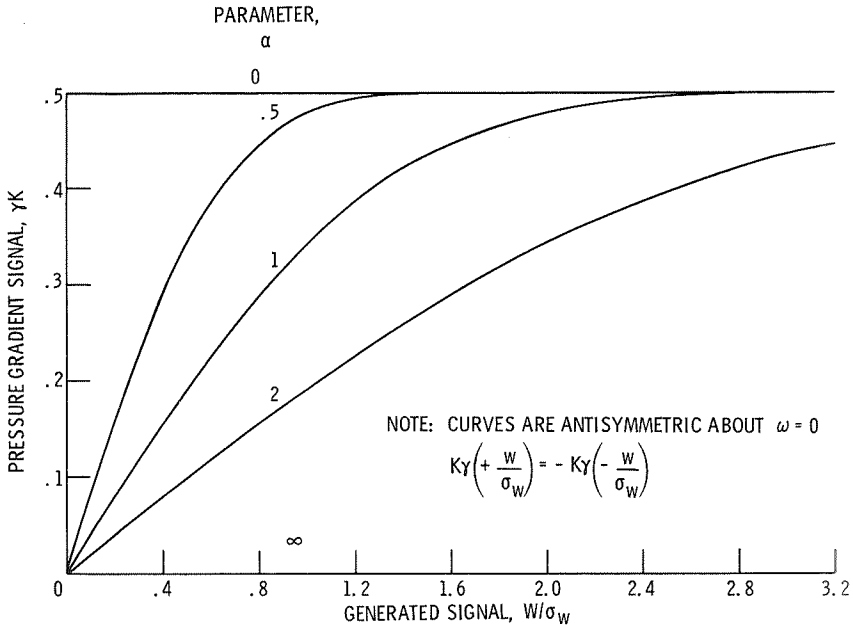

Figure 3. - Nonlinear transformation of generated signal w to pressure gradient signal γ.

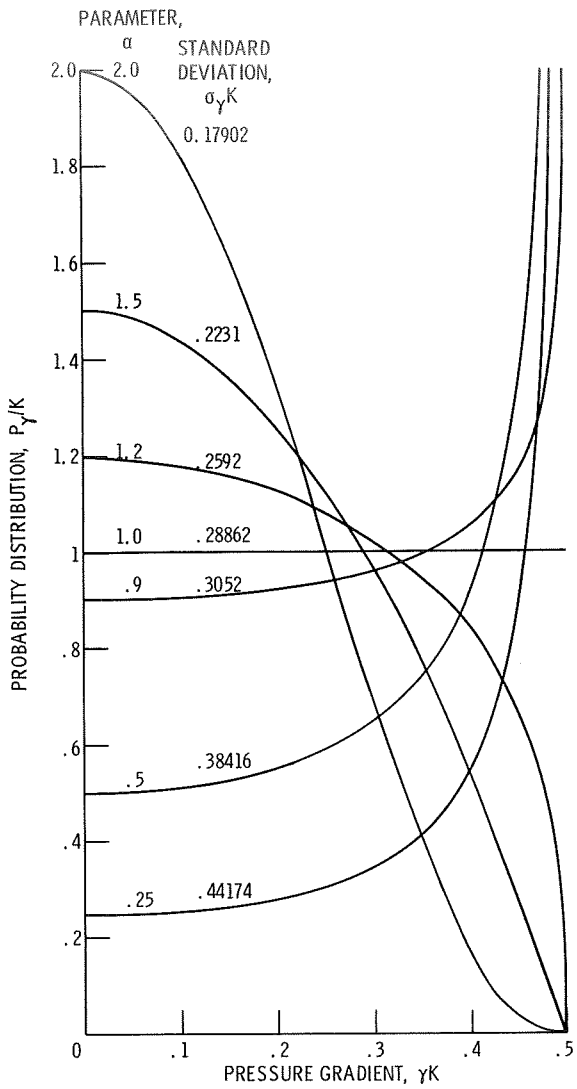

Figure 4. - Probability distribution of pressure gradient signal.

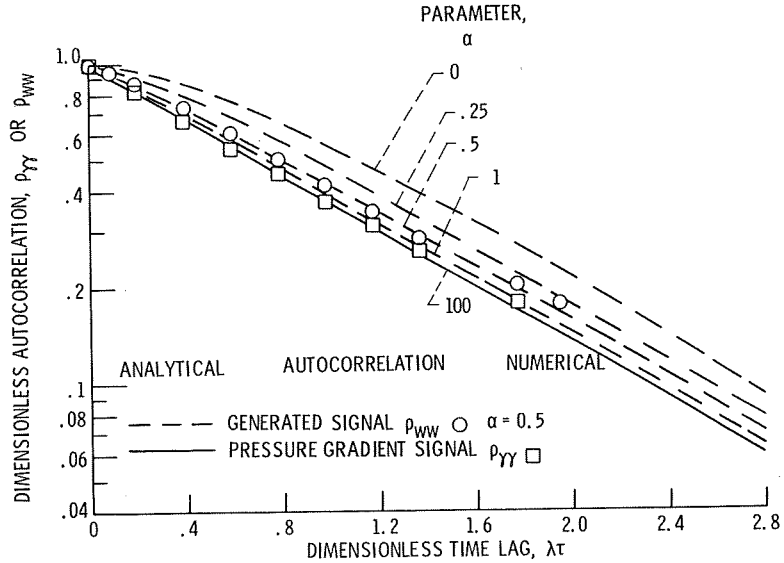

Figure 5. - Dimensionless auto correlations of generated signal and pressure gradient signal.

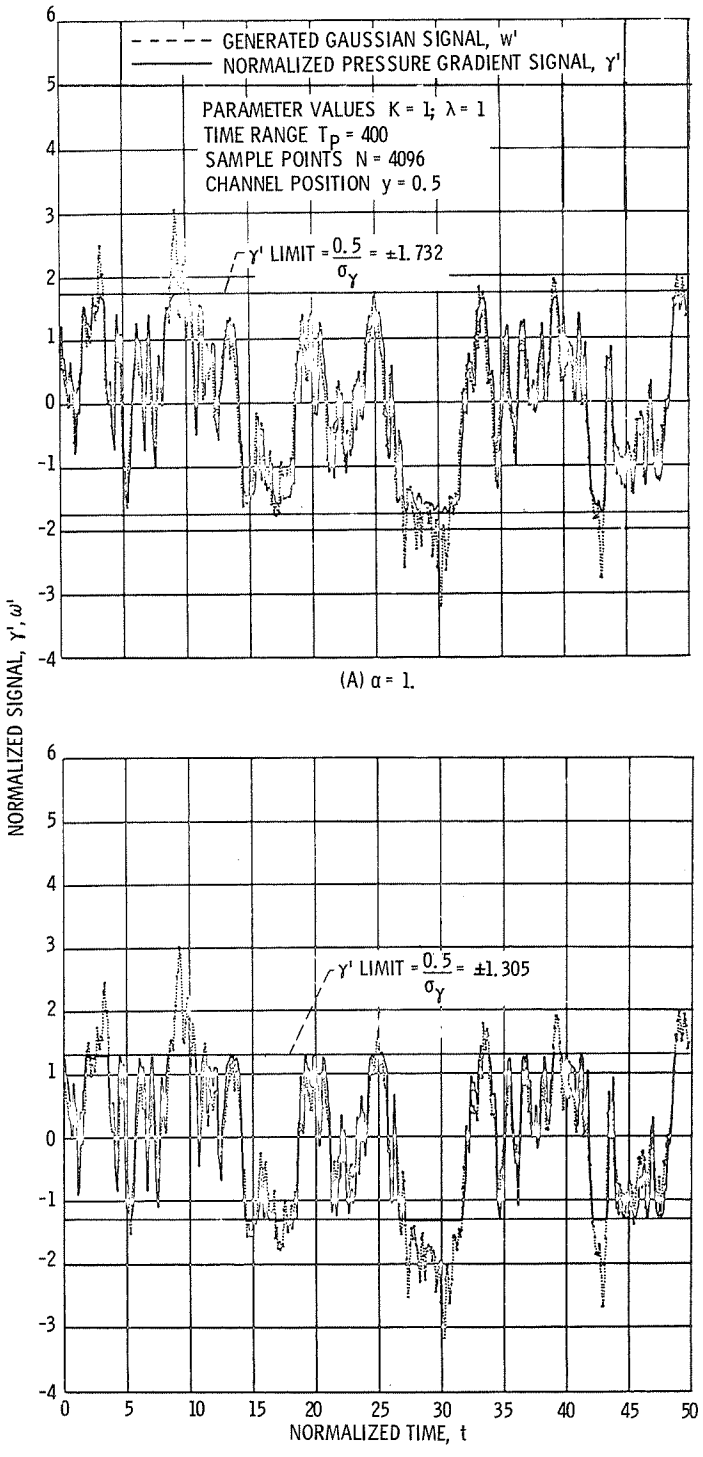

Figure 6. - Normalized generated Gaussian signal and pressure gradient signal.

E-6393

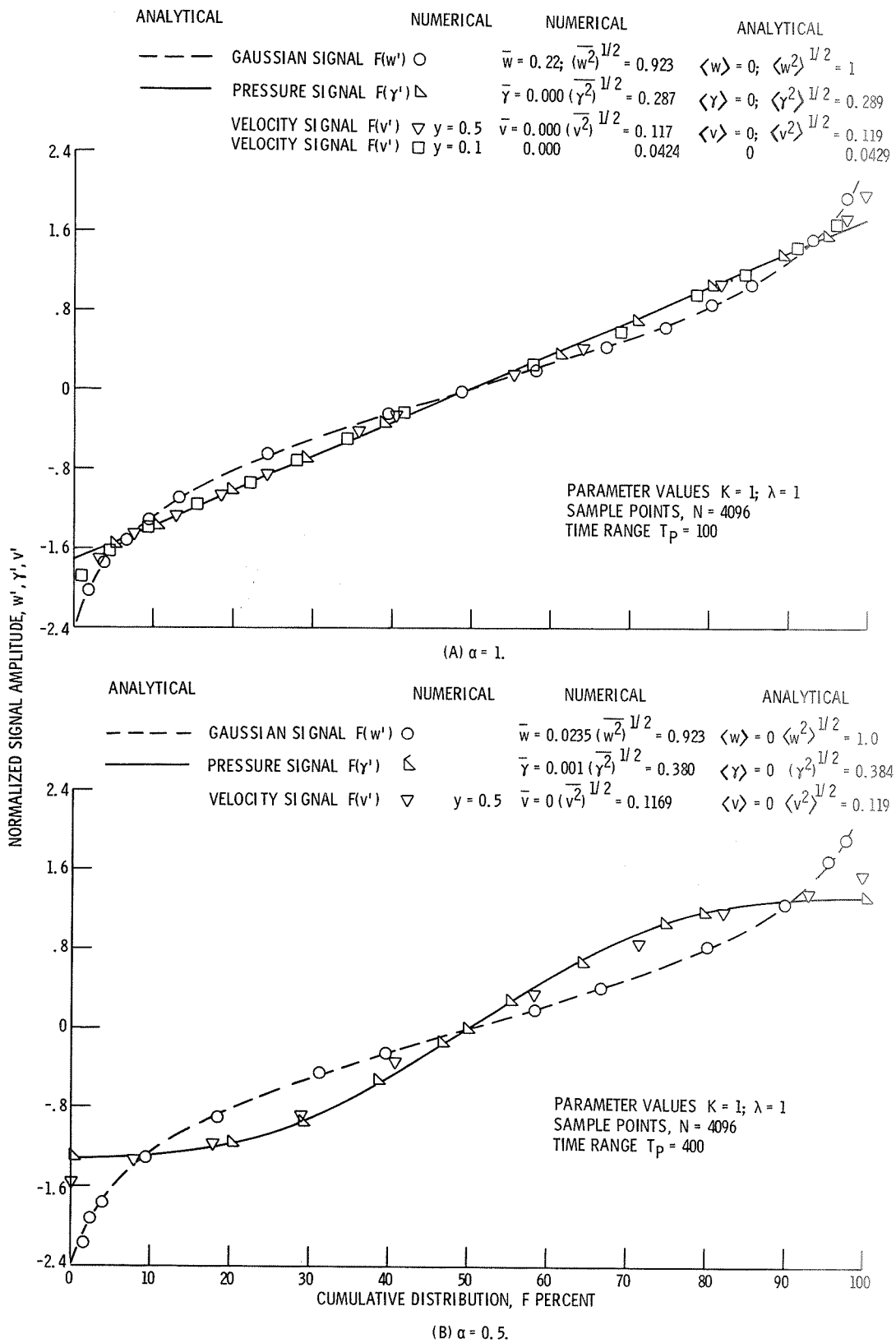

Figure 7. - Normalized cumulative distributions.

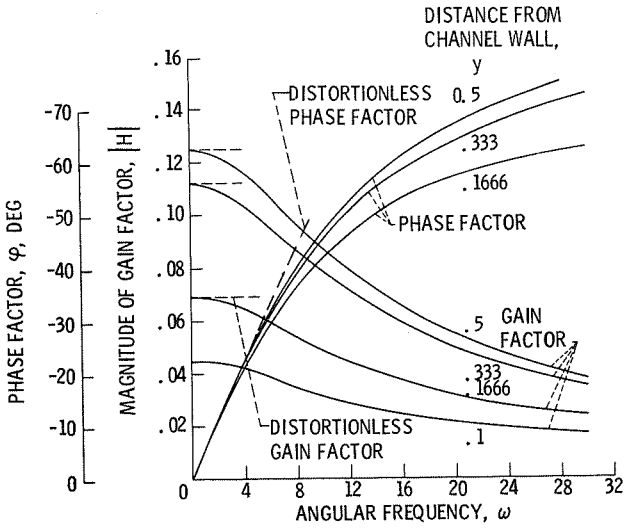

Figure 8. - System transfer function.

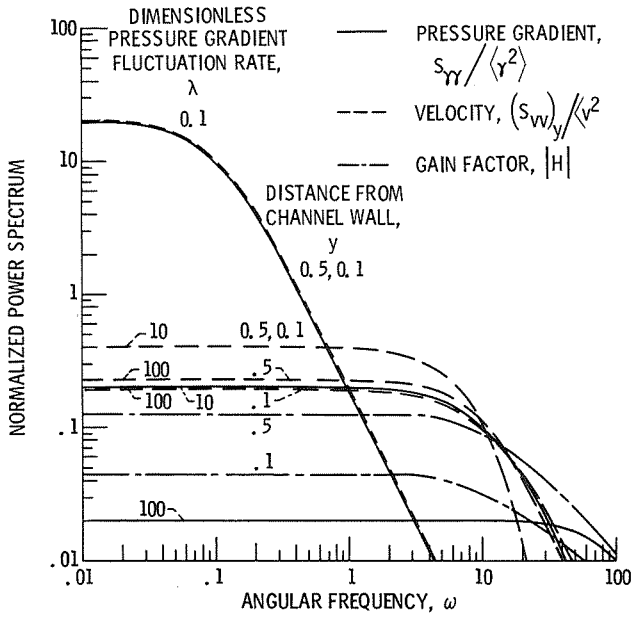

Figure 9. - Normalized power spectrums.

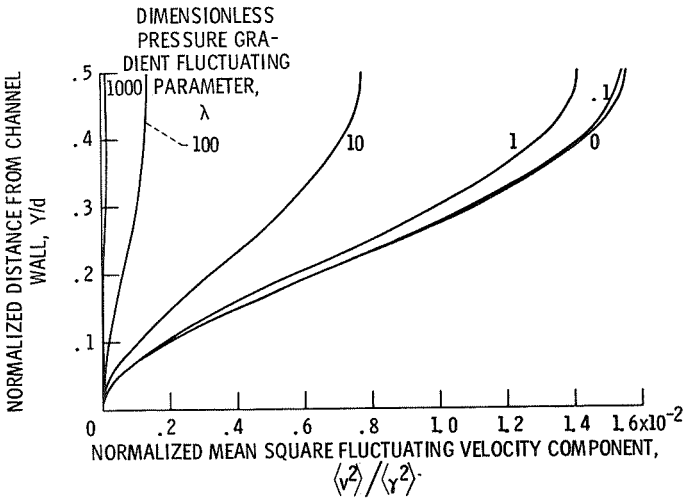

Figure 10. - Normalized mean square fluctuating velocity component across channel.

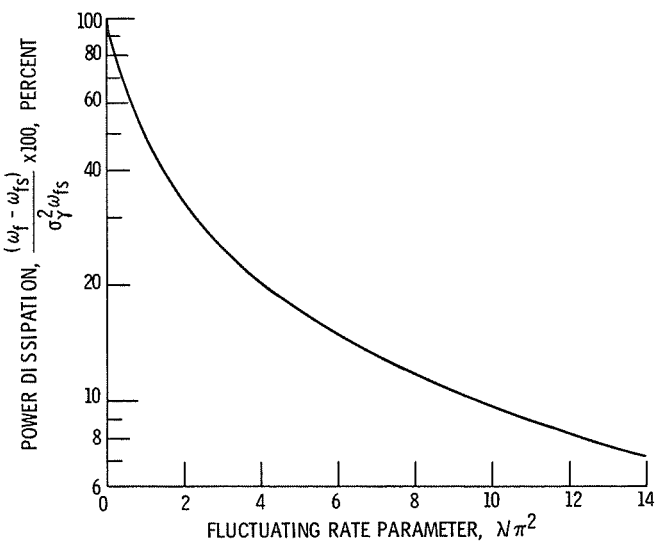

Figure 11. - Percentage increase in power dissipation ratio due to flow fluctuations.

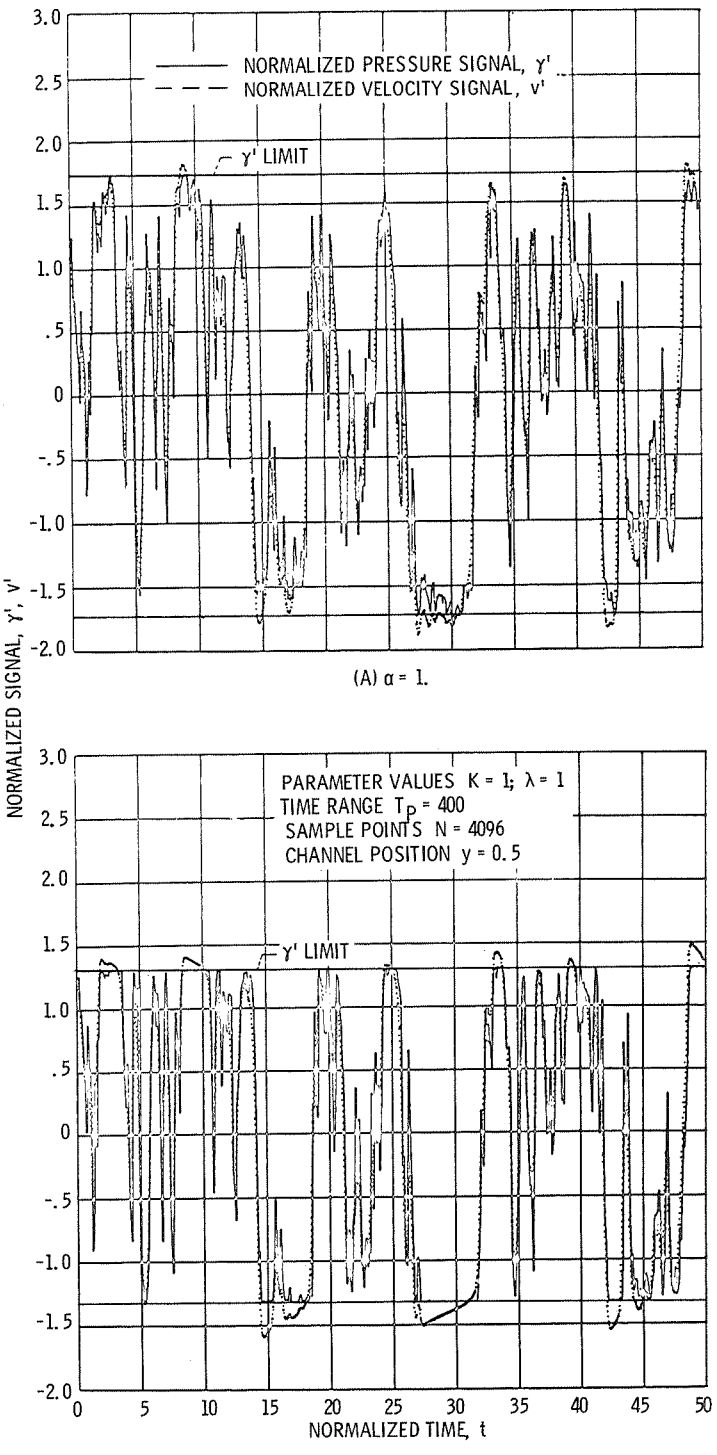

Figure 12. - Normalized pressure gradient and velocity signal.

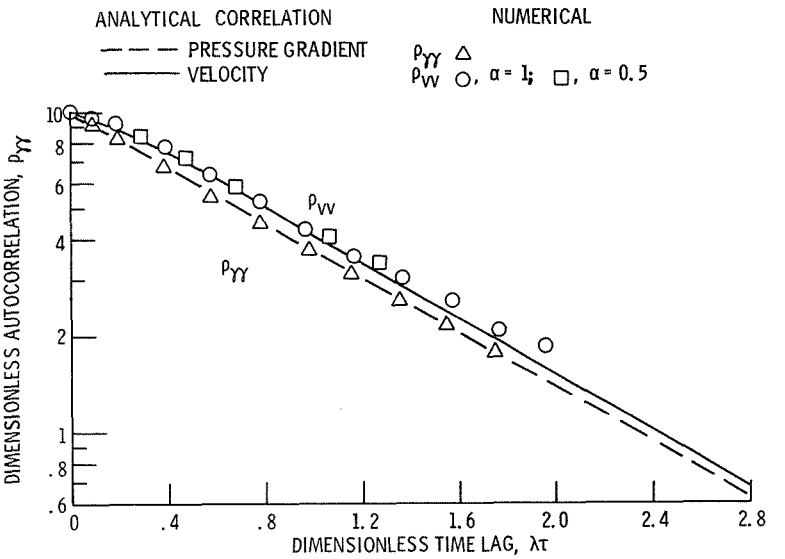

Figure 13. - Dimensionless autocorrelation of pressure gradient and velocity signal.